ON COMPUTATIONAL MODELING OF INTERACTIVE WIND AND ICING EFFECTS ON OVERHEAD LINE CONDUCTORS

Hooman Keyhan[1], Ghyslaine McClure[1], Wagdi G. Habashi[2]
[1]Department of Civil Engineering and Applied Mechanics, McGill University
[2]Computational Fluid Dynamics Laboratory, Department of Mechanical Engineering, McGill University
Montreal, Quebec, Canada
Hooman.Keyhan@mail.McGill.ca

Abstract: Transmission line analysis methods generally consider wind effects on conductors and supports as quasi-static loads, despite the dynamic nature of wind loading. In this paper, the authors explore wind-cable interactions using a 2-D fluid-structure interactive model using linear dynamic finite element analysis. The numerical simulation results reported show the effect of ice accretion thickness and bare conductor roughness on the resultant aerodynamic forces induced on the iced section.

1. INTRODUCTION

Design wind loads on overhead transmission line systems are usually considered as quasi-static horizontal loading resulting from a static pressure adjusted to account for drag effects. Hence, aerodynamic wind-cable interaction effects are only roughly approximated in design. Even though fluid-structure interaction (FSI) analysis is becoming fairly common in several engineering fields such as aerospace, automotive and biomedical applications, it has not been as frequently used in transmission line engineering. In this work, FSI analysis is used to study the wind-cable interactions in overhead transmission conductors and to explore the variation in the aerodynamic properties of conductors due to glaze ice accumulation. In current analysis methods, the wind-on-conductor load for iced conductors is simply obtained by adjusting the bare conductor load to account for the additional windward area. This approach negates the effects of the accretion on the drag and lift coefficients of the iced conductor. The general goal of this research is thus to develop a rational gusty wind load model for overhead conductors, in both iced and bare conditions, that will serve to determine the resultant wind forces acting at the tower attachment points. As a first step, the main focus of this paper is to illustrate how the conductor aerodynamic properties (drag and lift coefficients) change with ice thickness accumulated on the conductor.

2. RESULTS AND DISCUSSION

Figs. 1 and 2 display the effect of ice accumulation on the resulting drag and lift force coefficients of conductors with ice accumulation at the bottom edge, taking an ovoid shape with the major axis normal to the incident wind flow.

These force coefficients are determined from integration of the surface tractions exerted by the fluid flow on the interface between the fluid and solid domains. As vortices are shed in the wake, the aerodynamic forces fluctuate in time and the range of the calculated drag and lift is shown in the figures. The detailed paper presents the simulation results obtained for five different cable-ice geometries.

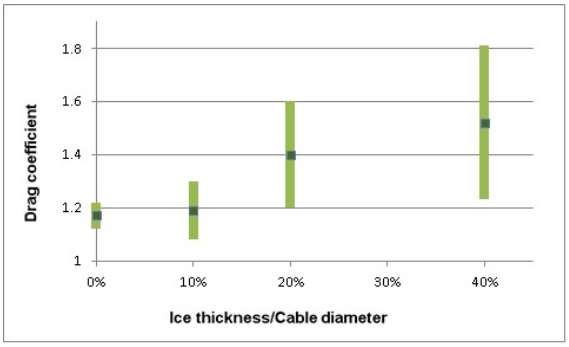

Figure 1: Effect of ice thickness accretion on drag coefficient

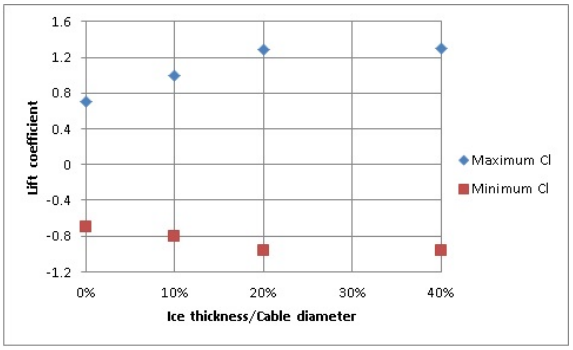

Figure 2: Effect of ice thickness accretion on lift coefficient

3. CONCLUSION

The study confirms that the shape of the iced cable is a significant factor on the effective wind loading, as the eccentric iced profile is subjected to larger net forces and motion. The eccentricity of the iced cable shape contributes significantly to the additional aerodynamic damping.

The smooth round and the stranded conductor shapes differ in their response with the stranded shape, experiencing drastically less forces and motion especially in vertical direction.

4. REFERENCES

[1] ADINA Inc (2009). ADINA theory and modeling guide. 71 Elton Ave, Watertown, MA 02472, USA.

[2] Bathe, K.-J. and H. Zhang (2002). "A flow-condition-based interpolation finite element procedure for incompressible fluid flows. *Computers & Structures*, **80**(14-15): 1267-1277.

On computational modeling of interactive wind and icing effects on overhead line conductors

Hooman Keyhan[1], Ghyslaine McClure[1]
[1]*Department of Civil Engineering and Applied Mechanics*
McGill University
Montreal, Quebec, Canada

Wagdi G. Habashi [2]
[2]*Computational Fluid Dynamic Laboratory, Department of Mechanical Engineering*
McGill University
Montreal, Quebec, Canada

***Abstract*— Current transmission line analysis methods generally consider wind effects on conductors and supports as quasi-static loads, despite the dynamic nature of wind loading. In this paper, the authors explore wind-cable interactions using a two-dimensional dynamic fluid-structure interactive model using linear dynamic finite element analysis. The numerical simulation results reported show the effect of ice accretion thickness and bare conductor roughness on the resultant aerodynamic forces induced on the iced cable section.**

Keywords- computational fluid dynamics; interactive wind and ice effects; overhead line conductors, conductor lift and drag coefficients; fluid-structure interactions

I. INTRODUCTION

Design wind loads on overhead transmission line systems are usually considered as quasi-static horizontal loading resulting from a static pressure adjusted to account for drag effects. Hence, aerodynamic wind-cable interaction effects are only roughly approximated in design. Even though fluid-structure interaction (FSI) analysis is becoming fairly common in several engineering fields such as aerospace, automotive and biomedical applications, it has not been as frequently used in transmission line engineering. In this work, FSI analysis is used to study the wind-cable interactions in overhead transmission conductors and to explore the variation in the aerodynamic properties of conductors due to glaze ice accumulation. In current analysis methods, the wind-on-conductor load for iced conductors is simply obtained by adjusting the bare conductor load to account for the additional windward area. This approach negates the effects of the accretion on the drag and lift coefficients of the iced conductor.

The general goal of this research is thus to develop a rational gusty wind load model for overhead conductors, in both iced and bare conditions, that will serve to determine the resultant wind forces acting at the tower attachment points. As a first step, the main focus of this paper is to illustrate how the conductor aerodynamic properties (drag and lift coefficients) change with ice thickness accumulated on the conductor.

II. MODELING APPROACH

The conductor used in the numerical simulations is a stranded ACSR 26/7 (Aluminum Conductor Steel Reinforced) with 29.5-mm outside diameter (D). As shown in Fig.1, five different shape conditions are modeled: (a) a circular smooth cylinder, (b) the realistic wavy surface profile of the bare stranded cable, (c) the stranded cable with a thin layer of ice accumulated at the bottom, (d) a smooth cylinder of oval shape representing a 6-mm thick layer of ice at the bottom, and (e) a smooth cylinder of oval shape with 12-mm ice thickness.

Model (a) serves to compare the results from this study with existing experimental test results that are mostly obtained on smooth circular cylinders. In model (b), the cable outline takes the shape of the contour of the 16 aluminum outer wires of 5-mm diameter each. In model (c) the maximum ice thickness is 3 mm (10% of the cable diameter) and the cable strands are still represented at the top surface. In models (d) and (e) the maximum ice thickness is increased to 20% and 40% of the cable diameter, respectively, at the bottom and the top surface of the conductor is assumed to be completely covered by ice, resulting in a smooth oval cross-sectional shape. As shown schematically in Fig. 1, the incident wind flow is assumed uniform and horizontal.

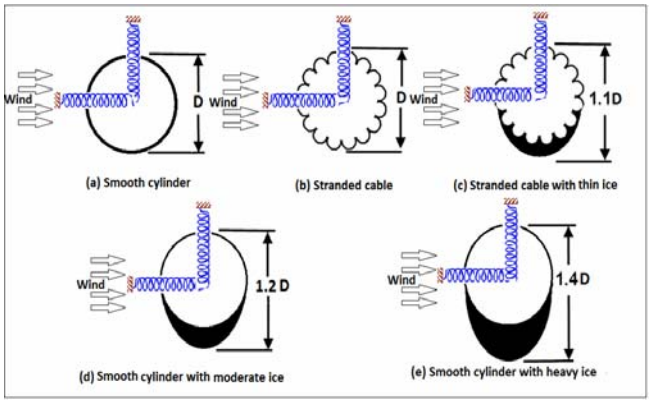

Figure 1. Five different cable sections under study .

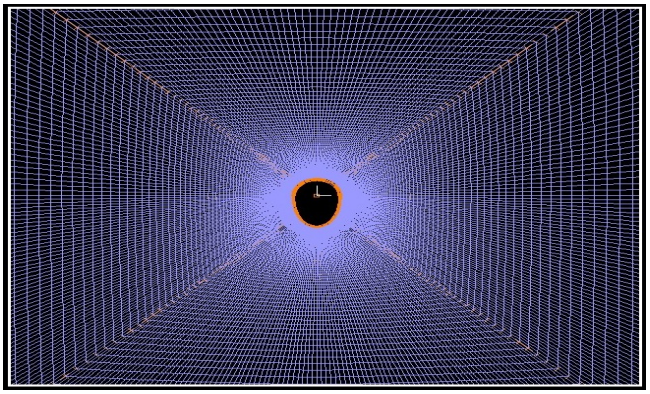

Figure 2. Part of fluid domain structured "O" mesh

The equivalent vertical and horizontal linearized stiffnesses of the conductor section are modeled by linear springs at the cable's centroid. These equivalent spring stiffness properties were determined for a mid-span cross-section using nonlinear elastic static analysis of a level 356-m span suspended in still air with fixed ends, with a horizontal tension of 19.2 kN in the bare condition (cable self-weight 14.9 N/m), and 22.5 kN in the iced condition (iced cable weight 17.9 N/m). A small viscous damping constant (equivalent to 1% of critical) is also assigned at the support in each orthogonal direction to approximate internal material damping effects in the conductor.

As previously reported [2], the overall dimensions of the fluid domain had to be optimized for CFD and FSI analyses to ensure that the computational domain is large enough for the fluid boundaries to have negligible effects on the calculated cable response, and yet attempt to reduce the computational cost. The fluid domain (see Fig. 2) has a horizontal length of 60xD and a vertical depth of 40xD. Further fluid modeling considerations are discussed next.

III. DETAILED MODELING CONSIDERATIONS

To keep the cable cross-sectional model simple, only the outer cable boundary is modeled using stiff two-dimensional Bernoulli beam elements with appropriate tributary mass. To get a smooth geometric profile and retain reasonable accuracy in FSI analysis, the perimeter of the conductor is modeled with beam elements of length varying between 0.30 to 0.32 mm (300 to 380 elements in total) in the different models. In the solid domain, the incremental form of the nonlinear equations of motion (updated Lagrangian formulation) of the cable cross section on spring supports with dashpots is solved by direct integration using the classical unconditionally stable Newmark method, and the equilibrium iterations are carried out using the Full Newton method for stiffness updates [1].

The fluid domain is discretized with quadrilateral FCBI-C elements [3] using a structured "O" shape mesh, as shown in Fig.2 **错误！未找到引用源。** for cable section (e). Using the FCBI-C elements, the degrees of freedom of the fluid elements are defined at the centroid and the solution variables are piecewise constant. The final solution is interpolated at corner nodes for post-processing purpose. Discretizing the fluid domain with these elements helps reach stability for different Reynolds number without setting any artificial numerical parameters [3].

The fluid mesh geometry that provided optimal computational performances differs for each case, ranging from 90 × 75 to 120 × 106 elements at the external boundaries for the circular cylinder (a) and the more heavily iced cylinder (e), respectively. The fluid mesh is gradually refined to a resolution of 300 to 380 elements at the air-cable interface. The refined mesh in a ring zone of about 1xD thickness around the cable surface (see Fig. 2) is able to capture the response with reasonable accuracy. Cell thicknesses around the solid domain are small enough to allocate about 5 mesh layers with a Y^+ under 10.

The CFD analysis proceeds with direct time integration of the unsteady Reynolds-averaged Navier-Stokes equations using the Euler α - method of first order, and a constant time step of 0.1 ms was found optimal for the problem at hand. The iterative solver for the linearized incremental equations is the Algebraic Multigrid method (AMG). Airflow turbulence is modeled with the Spalart-Allmaras one-equation model and vortex-shedding effects are introduced with the Detached Eddy Simulation (DES) algorithm. In FSI analysis, the Arbitrary-Lagrangian-Eulerian (ALE) formulation is used to allow for compatible mesh deformations and displacements for the fluid surrounding the cable in motion in each solution step. [1]

IV. RESULTS

For the sake of brevity, only the salient features of the results obtained for the five models with incident wind speeds of 20 and 10 m/s are presented next. Fig. 3 shows the calculated pressure fields developed around the cable in the five models subjected to the same incident flow conditions at time t = 2 s. The pressure fields show the largest fluctuations in the heavy iced cylinder case (Fig. 1e) and the smallest for the bare stranded cable (Fig. 1b), while the smooth circular cylinder (Fig. 1a) yields intermediate results. The maximum pressure developed at the stagnation point reaches 266 Pa in the heavily iced cylinder, 235 Pa and 232 Pa in the bare stranded cable and smooth circular cylinder, respectively.

The negative pressure on the leeward side of the heavily iced cylinder reaches -930 Pa compared to -454Pa in the bare stranded cable. The pressure fields are significantly different for the five models considered: the heavily iced cylinder experiences the largest area of the negative pressure zone, from the flow separation point to the leeward side, followed by the iced and bare circular cylinders, and finally the stranded cable profile experiences the smallest suction area. The stranded cable shows round improved aerodynamic behavior compared to cylinder, as its corrugated surface enables a more gradual flow separation [2]. These differences in pressure explain the trends observed in cable response, which are discussed next.

Figs. 4 and 5 present time history plots of the net cable force response calculated from the integration of the

pressure field at the air-cable interface. The force response of the five models is shown in terms of drag (C_D in Fig. 4) and lift (C_L in Fig. 5) coefficients. The heavily iced cable model, with its eccentric shape, experiences the largest drag coefficient with a value of 1.82 in the steady state; followed by the moderately iced cylinder with 1.5, and the circular cylinder has the smallest value, slightly below 1.2. The drag forces oscillate with a frequency of 59 Hz, which corresponds to a Strouhal number value of about 0.18.

Fig. 5 compares the vertical force response and it is seen that the heavily and moderately iced cylinders present similar behavior (C_L= +1.2 ~ C_L= -1.0), while the stranded cable is significantly less loaded with $C_L \approx \pm 0.7$.

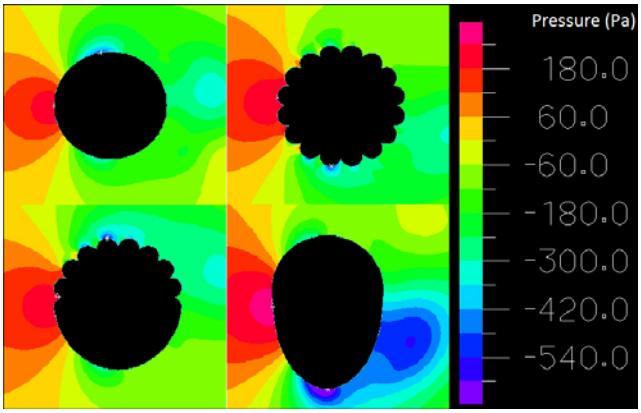

Figure 3. Pressure fields around the cable in four models (t = 2 s; incident wind speed = 20 m/s; ρ = 1.22 kg/m^3, and μ = 1.7×10-5 kg/m.s)

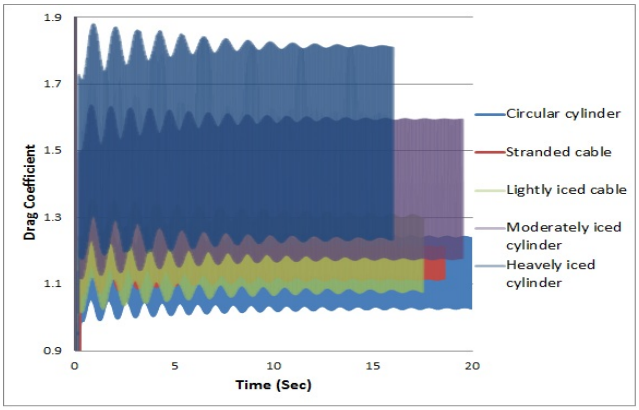

Figure 4. Drag coefficient obtained from different models for V=10m/s

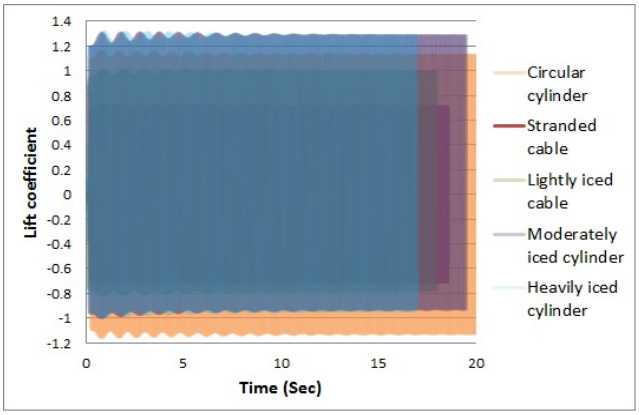

Figure 5. Lift coefficient obtained from different models for V=10m/s

V. EFFECT OF ICE ACCRETION ON DRAG AND LIFT COEFFICIENTS

Analysis results for all five models with different ice thickness values confirm that the aerodynamic properties change significantly with ice thickness. Of course, the orientation of the incident wind flow is also an important factor, but the results discussed here are strictly for the wind flow direction indicated in Fig. 1. Figs 6 and 7 display the variations in drag and lift coefficients, respectively, for different amounts of ice accumulation.

As expected, the drag and lift coefficients increase with ice accumulation, particularly when the ice thickness is increased from 10% of cable diameter to 20%, but this also includes the influence of the change in the top surface roughness (see Fig. 1c and d). In most experimental works, the drag and lift coefficients are reported as constant values developed at the steady-state. However, the numerical results show that the magnitude of the drag and lift forces is fluctuating by as much as 30% depending on ice thickness and wind velocity. As shown in Figs. 4 and 6, the amplitude of the drag force fluctuations increases with ice thickness because of the larger fluctuations induced in the pressure field for the more asymmetric profiles. Fig.7 shows that the lift coefficient seems to stabilize with the increased ice thickness when the iced shape takes similar eccentric ovoid profiles (see Fig. 1 d and e).

Fig. 8 displays the cable horizontal displacement history for the five different models. It is seen that the steady state is reached after about 15 s and the transient amplitude is about twice the steady-state value. Again, in keeping with the preceding results, the heavily iced cable experiences the largest motion and the stranded cable, the smallest. Fig. 8 also provides useful information on the amount of aerodynamic damping present in the five models when the logarithmic decrement of the amplitude of the transient motion is calculated. In the particular flow conditions of the cases reported here, the viscous damping ratios are approximately 3.5% for the iced cylinder, 2.3% for the stranded cable and 1.6% for the smooth bare cylinder.

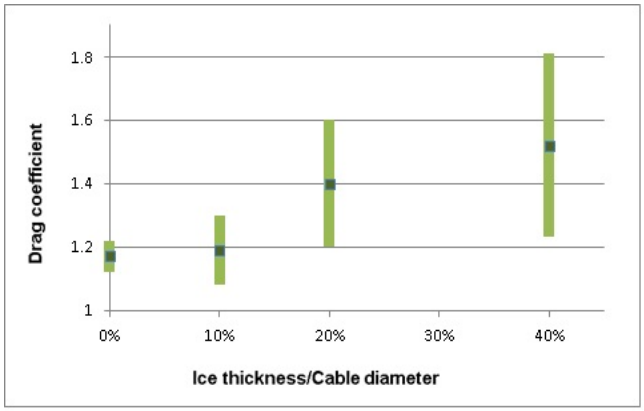

Figure 6: Cable drag coefficient for different ice accumulations

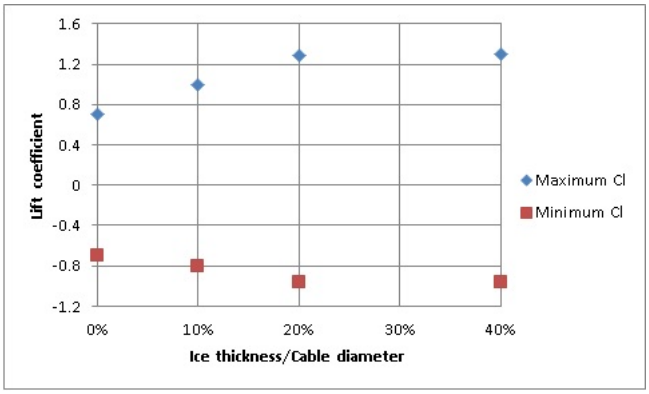

Figure 7: Cable lift coefficient for different ice accumulations

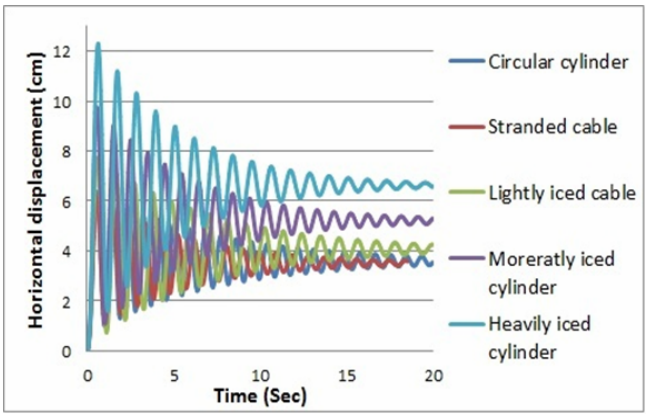

Figure 8: Horizontal displacement with wind incident of V=10m/s

Recalling that the cable elastic supports already accounted for the presence of dashpots with viscous damping ratio of 1%, it is seen that the eccentricity of the iced cable shape contributes greatly to the additional aerodynamic damping.

VI. CONCLUSION

A computational study of the dynamic wind-cable interactions on two-dimensional models of five bare and iced cable cross-sectional shapes reveals that, unlike most of the results reported from experimental studies and used in design, drag and lift coefficients are not constant for the cable as resultant forces fluctuate due to both wind-cable interaction and vortices in the flow around the cable. Depending on cable movement, wind speed and cable shape, the amplitude of these fluctuations may be as large as 50% of its maximum value. In this study, the incident wind direction was fixed and it was confirmed the cable shape alone is a significant factor on the wind-induced cable response. As expected, the eccentric iced shape is subjected to larger net forces and motion. The presence of a thin layer of ice causes a significant increase on lift forces but when the ice thickness exceeds 40% of the cable diameter the lift remains almost unchanged (the asymmetric aerodynamic shape remains similar) while the drag force still increases significantly due to the increased drag coefficient and the larger windward area of the iced cable.

Overall, the smooth round cylinder and the bare stranded conductor shapes differ significantly in their response, with the stranded conductor experiencing significantly less forces and motion than the smooth round cylinder, especially in the vertical direction. Although the results obtained for other incident wind velocities were not presented, similar trends have been observed and the differences in response observed here were found to be exacerbated at lower wind speeds.

ACKNOWLEDGMENT

A research team grant from the Fonds québécois de la recherche sur la nature et les technologies (FQRNT) is kindly acknowledged.

REFERENCES

[1] ADINA Inc (2009). ADINA theory and modeling guide. 71 Elton Ave, Watertown, MA 02472, USA.

[2] Keyhan, H., McClure, G., Habashi,W.G. (2010). Computational study of surface roughness and ice accumulation effects on wind loading of overhead line conductors. 13th International Conference on Wind Engineering (ICWE13). Amsterdam, The Netherlands, 10-15 July 2011.

[3] Bathe, K.-J. and H. Zhang (2002). A flow-condition-based interpolation finite element procedure for incompressible fluid flows. *Computers & Structures*, **80**(14-15): 1267-1277.